

## Enhancement of the Production Rate in Chemical Reactions with Thresholds

W. Hohmann, D. Lebender, J. Müller, N. Schinor, and F. W. Schneider\*

Institute of Physical Chemistry, University of Würzburg, Am Hubland D-97074 Würzburg, Germany

Received: July 11, 1997<sup>⊗</sup>

In nonlinear chemical reactions with threshold properties, exceptionally large enhancements of the production rate in a chemical flow reactor may be achieved by external periodic forcing. A threshold may be represented by the turning point in a bistability curve or by a Hopf bifurcation between a focal steady state and a limit cycle. Since the production rate is equal to the (mathematical) product of the flow rate and the reaction yield, large production rate enhancements will be achieved at high flow rates with short pulses to lower flow rates if the product yield increases with decreasing flow rate into the reactor. Sinusoidal flow rate perturbations and perturbations using short pulses give equally large production rate enhancements over the free running reaction if the comparison is made at the same average flow rate. If the comparison is made for identical perturbation amplitudes, the pulse perturbations lead to larger production rate enhancements than the sinusoidal perturbations. An easy way to achieve unusually large production rate enhancements ( $\sim 100\%$ ) is to simply turn the flow rate periodically on and off in analogy to the bang-bang method. This is demonstrated experimentally in the minimal bromate oscillator using a subcritical Hopf bifurcation as a threshold and by corresponding NFT model calculations.

### Introduction

One of the important goals in chemical synthesis is the optimization of product formation from a given amount of reagents. A vast literature exists<sup>1–18</sup> dealing with the cyclic operation of chemical reactions in open systems. In this work we focus our attention to a nonlinear chemical reaction with threshold properties, which shows a dramatic enhancement in the rate of product formation when the threshold is periodically crossed by a control variable such as the flow rate in an isothermal continuous flow stirred tank reactor (CSTR). A threshold may be represented by a subcritical Hopf bifurcation as in the present minimal bromate oscillator or by a turning point of a bistability at which the (average) product concentration changes substantially.

The rate of product formation (or production rate PR) may be enhanced by operating at increased flow rates and yields, since PR is proportional to the (mathematical) product of the flow rate ( $k_f$ ) and the product concentration. However, if the reaction yield decreases with increasing  $k_f$  as in the bifurcation diagram of the minimal bromate oscillator (Figure 1a), a simultaneous increase of both the product concentration and the flow rate is not possible. Instead, a periodic operation is suggested that carries the high yield advantage (at low  $k_f$ ) for a sufficiently long time into the high- $k_f$  region where the  $k_f$  term makes a large contribution to the PR. Thus, large PR enhancements may be produced. These enhancements may be compared for two types of modulations of the flow rate, namely for sinusoidal and pulsed modulations either at the same *average* flow rate or at the same flow amplitudes. Another possibility is to switch the flow rate periodically on and off in a bang-bang-like fashion. This simple procedure turns out to be the most efficient way to enhance the rate of product formation in the present system. The bang-bang control strategy is known to be optimal<sup>22</sup> for control problems that are linear in the control variables such as in the flow rate into a CSTR.

Thus, in threshold systems, average experimental production rates are dramatically enhanced over the maximum production

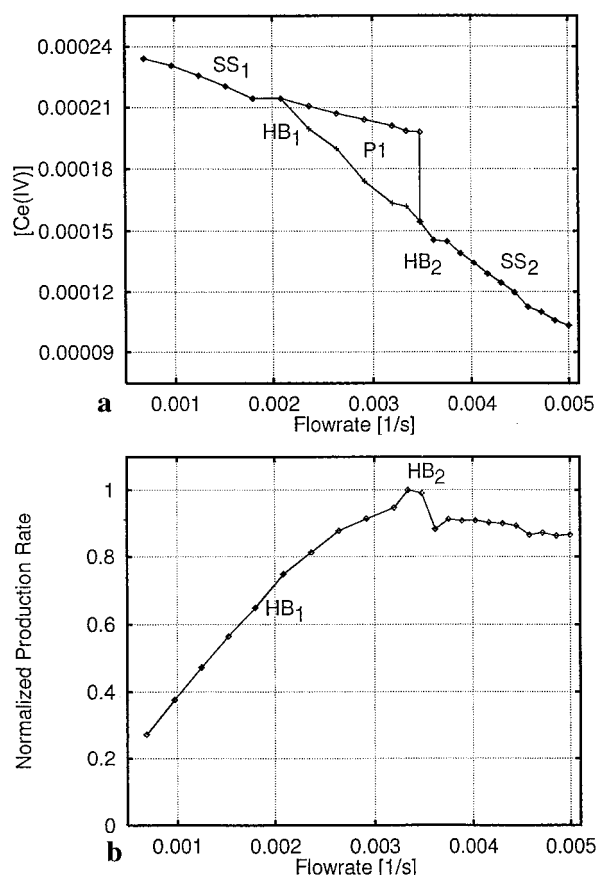


**Figure 1.** (a) Experimental bifurcation diagram of the MB reaction: Ce(IV) concentration versus flow rate. SS<sub>1</sub> (focal steady state), HB<sub>1</sub> (supercritical Hopf bifurcation), P<sub>1</sub> (oscillations of period one), HB<sub>2</sub> (subcritical Hopf bifurcation), and SS<sub>2</sub> (focal steady state). (b) Normalized production rate versus flow rate in the autonomous MB reaction. The normalized average production rate PR displays an almost linear increase with increasing  $k_f$ . A maximum ( $k_f \approx 0.0033 \text{ s}^{-1}$ ) is observed close to HB<sub>2</sub>, which we normalize to unity (values exceeding unity represent enhancements (Figures 2–5)). In the focal steady state SS<sub>2</sub>, the production rate is lower than unity due to the declining [Ce(IV)] (Figure 1a).

<sup>⊗</sup> Abstract published in *Advance ACS Abstracts*, November 15, 1997.

rate in the free running CSTR mode or over any periodically driven state in which a threshold is not crossed as we demonstrate with experiments using the minimal bromate reaction (MB)<sup>19</sup> and the corresponding Noyes–Field–Thompson (NFT) model.<sup>20</sup> The MB reaction describes the oscillatory interconversion between Ce(III) and Ce(IV) in the presence of bromate and bromide in sulfuric acid solution. It represents the inorganic part of the Belousov–Zhabotinsky reaction, and its mechanism is well understood.<sup>20,21</sup> Together with bromate and bromide, Ce(III) is one of the educts and Ce(IV) is considered to be one of the products of the reaction that takes place in a continuous flow stirred tank reactor.

### Production Rate

The production rate is defined as the mathematical product of the flow rate  $k_f$  and the product concentration [Ce(IV)] at the particular flow rate. Its dimension is mol/(L s). Since the PR may be measured in the effluent of the CSTR, its value is zero when  $k_f = 0$ , i.e., when the reaction occurs in the batch. However, the batch system is not of any interest here. Since neither the product concentration (yield) nor the flow rate remain constant during the flow perturbations, the average PR ( $PR_{av}$ ) is calculated according to

$$PR_{av} = \frac{1}{N} \sum_{i=1}^N k_{f_i} \cdot [Ce(IV)]_i \quad (1)$$

where  $N$  is the number of experimental ( $\sim 1100$  per single experiment) and theoretical ( $\sim 50\,000$  per single simulation) data points, respectively.

### Comparisons of PR Enhancements

The enhancement of the production rate for sinusoidal and for pulsed flow rate perturbations may be compared either at the same flow frequency and flow amplitude or, more commonly, at the same average flow rate. However, a comparison at the same average flow rate will require large sinusoidal amplitudes that are difficult to be realized experimentally in our system. Therefore we carry out the comparisons at the same average flow rates only in our NFT model simulations.

### Experimental Section

A shortened spectrophotometric cell (1 cm path length) serves as a CSTR<sup>18</sup> (1.5 mL volume, 25.0 °C). A precise syringe pump (regulated by a computer via a DA/AD converter) delivers three reactant feed streams that enter through a Teflon stopper: sulfuric acid (1.5 M), cerous(III) sulfate ( $3 \times 10^{-4}$  M) and potassium bromide ( $4.0 \times 10^{-4}$  M), and potassium bromate (0.10 M) as reactor concentrations. The outflow occurs through a tube in the middle of the stopper. The stirring rate is 1200 rpm. Data are computer-collected at 1 Hz. The Ce(IV) concentration is monitored spectrophotometrically at 350 nm.

### Results and Discussion

**Bifurcation Diagram, PR in the Free Running Mode.** The experimental bifurcation diagram summarizes the observed dynamic states (focal steady states  $SS_1$  and  $SS_2$ , limit cycle  $P_1$ ) in the autonomous MB reaction as a function of flow rate (Figure 1a). At a low flow rate ( $k_f = 0.0021 \text{ s}^{-1}$ ), there is a supercritical Hopf bifurcation ( $HB_1$ ) where the focal steady state  $SS_1$  changes into the oscillatory state  $P_1$ . The periods increase between 200 and 500 s with increasing flow rate. At a higher flow rate ( $k_f = 0.0034 \text{ s}^{-1}$ ), a subcritical Hopf bifurcation  $HB_2$  is observed. Here the oscillatory state changes into a focal steady state whose Ce(IV) concentration decreases with increasing  $k_f$ . It is

important to note that the region of coexistence of the oscillatory state and the focus at the subcritical  $HB_2$  turns out to be too narrow to be resolved experimentally in this case. This is in agreement with our NFT model simulations. The subcritical Hopf bifurcation represents the threshold for the “hard generation” of large amplitude Ce(IV) oscillations.

In the free running mode of the autonomous reaction (Figure 1a), the average production rate (eq 1) rises almost linearly and displays a maximum ( $k \approx 0.0033 \text{ s}^{-1}$ ) close to  $HB_2$  (Figure 1b), which we normalize to unity since we are interested in the enhancement above this value due to (later) periodic crossings of the threshold. Eventually, the production rate declines to zero at very high flow rates where product formation approaches zero. Therefore, the following production rate enhancements are compared with the maximum production rate at  $k_f \approx 0.0033 \text{ s}^{-1}$  in the free running mode unless otherwise indicated.

**Sinusoidal Modulation of the Flow Rate.** To achieve the desired enhancement of the Ce(IV) production rate, a flow rate modulation is introduced. Sinusoidal perturbations are applied to the flow rate  $k_f^0$  according to

$$k_f = k_f^0 (1 + \alpha \cdot \sin(\omega t)) \quad (2)$$

where  $k_f^0$  represents the constant average flow rate at a chosen focal steady state,  $\alpha$  is the amplitude of the sine function, and  $\omega$  is the frequency of the forcing function. In the following experiments (Figure 2), the average flow rate is chosen to be 19% ( $k_f^0 = 0.0040 \text{ s}^{-1}$ ) above  $HB_2$ . The modulation amplitude is chosen such that the flow rate crosses  $HB_2$  periodically into the oscillatory region (Figure 2a,c,e; for  $\alpha = 0.3$ ). As a consequence the chemical reaction responds with Ce(IV) oscillations of relatively high amplitude (Figure 2b,d,f). For perturbation periods of 125 s (Figure 2a) and larger, the system responds with one oscillation per perturbation period (1:1) (Figure 2b). For a shorter period (100 s) (Figure 2c) the system is still in the refractory state when the Hopf bifurcation is crossed for the subsequent time by the forcing function leading to a 1:2 response (Figure 2d), whereas a low perturbation period (50 s) (Figure 2e) leads to complex oscillations of lower period and larger amplitude.

**PR Enhancement.** The average production rate (Figure 4a) is high at perturbation periods for which the ratio between the response period and the perturbation period is 1:1. The higher the perturbation amplitude, the higher the production rate enhancement. The maximum PR enhancements are 21% at  $\alpha = 0.2$  ( $T = 200$  s) and 24% at  $\alpha = 0.3$  ( $T = 125$  s). For periods shorter than 200 s (125 s), the production rate enhancement declines between 200 and 175 s (between 125 and 100 s (Figure 2d)) for  $\alpha = 0.2$  ( $\alpha = 0.3$ ) since the above ratio changes to 1:2. An increase of the production rate follows until the system responds with complex oscillations at periods smaller than 100 s (50 s) for  $\alpha = 0.2$  ( $\alpha = 0.3$ ) for which the PR enhancement decreases.

**Pulsed Modulation of the Flow Rate.** The optimal perturbation function turns out to be a short rectangular pulse in  $k_f$ , since a (negative) pulse leads to a (short time) operation at a low flow rate  $k_{f \text{ min}}$  where the yield is high (Figure 1a) followed by a long-time operation at high flow rates  $k_{f \text{ max}}$ . This pulsed operation of the flow rate from  $k_{f \text{ min}}$  to  $k_{f \text{ max}}$  is analogous to the “bang-bang” method known in chemical engineering.<sup>22</sup> There are a number of parameters still to be optimized such as the pulse amplitude, the pulse length, the interval between two pulses, and the “distance” of the chosen focus from  $HB_2$  on the  $SS_2$  branch. It is evident that the calculated average flow rate in the pulsed mode increases with decreasing pulse length, where the pulse interval is the difference between the pulse period and the pulse length.

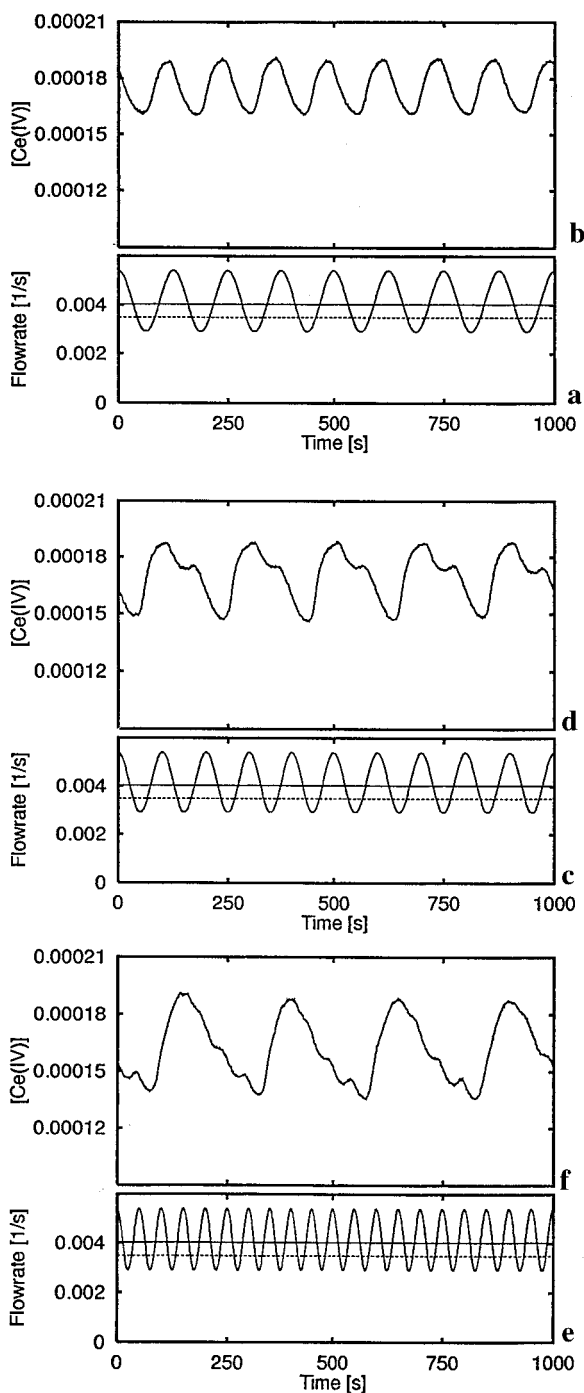


**Figure 2.** Sine perturbation functions of the flow rate with periods (a) 125 s, (c) 100 s, (e) 50 s and resulting time series (b, d, f) for  $\alpha = 0.3$  in the MB experiment at  $k_f^0 = 0.0040 \text{ s}^{-1}$ . At a lower amplitude ( $\alpha = 0.2$ ) the situation is qualitatively similar. The full line indicates the average  $k_f$ ; the dotted line indicates the position of  $HB_2$ .

For a comparison at the same flow amplitudes as in sinusoidal forcing we set the maximal  $k_f$  value equal to the maximal flow rate during the sine perturbation at  $\alpha = 0.3$  (55% above  $HB_2$ ) while the flow rate during the pulse ( $k_{f \text{ min}}$ ) is adjusted to be equal to the minimal flow rate of the corresponding sine function (17% below  $HB_2$ ) (Figure 3a,c). For short rectangular pulses a 1:1 response (Figure 3b) with a higher production rate enhancement (41%) than in the preceding sinusoidal operation (24%) (Figure 2b) is measured at an optimal pulse length (20 s) and pulse interval (100 s) (Figure 3a). Note that the time series of the response to the sine and the pulse perturbations show great similarities at identical perturbation frequencies (compare Figures 2b and 3b). The observed increase in the PR enhance-

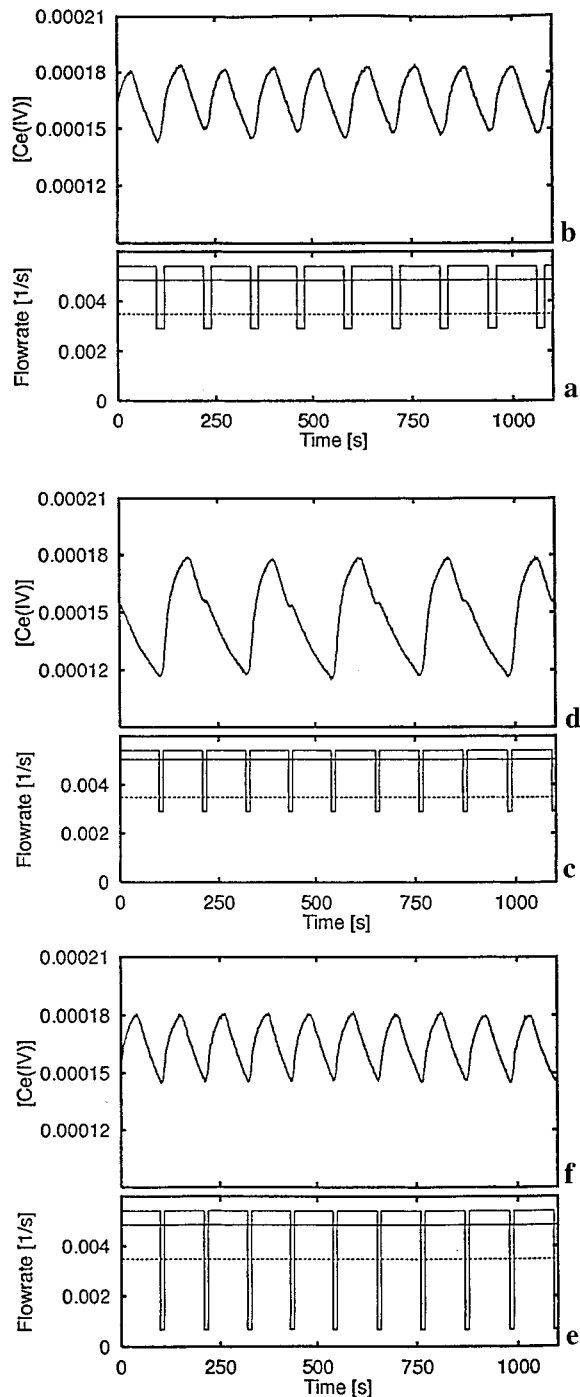


**Figure 3.** Short rectangular pulse perturbations (a, c, e) and resulting time series (b, d, f) in the MB experiment for pulse intervals 100 s (a). For a pulse length of 20 s, the response in (b) is one oscillation per perturbation period (1:1), PR enhancement 41%; (c) pulse length 10 s, response (d) is 1:2, PR enhancement 35%; (e) increased pulse amplitude (minimal  $k_f$  is 80% below  $HB_2$ ), response (f) is 1:1, PR enhancement 45%. The full line indicates the average  $k_f$ ; the dotted line indicates the position of  $HB_2$ .

ment is therefore due in large part to the higher average flow rate in the pulsed experiments (although the flow rate amplitudes are chosen to be identical for the sinusoidal and the rectangular perturbations in this case). For the shorter pulse length (10 s) (Figure 3c), the system is still in the refractory state when the Hopf bifurcation is crossed for a subsequent time leading to a lower production rate enhancement (35%) due to a change of the ratio between the response period and the perturbation period from 1:1 to 1:2 (Figure 3d). However, an increase in the perturbation amplitude (Figure 3e) restores the 1:1 ratio (Figure 3f) with a concomitant enhancement (45%) of the average

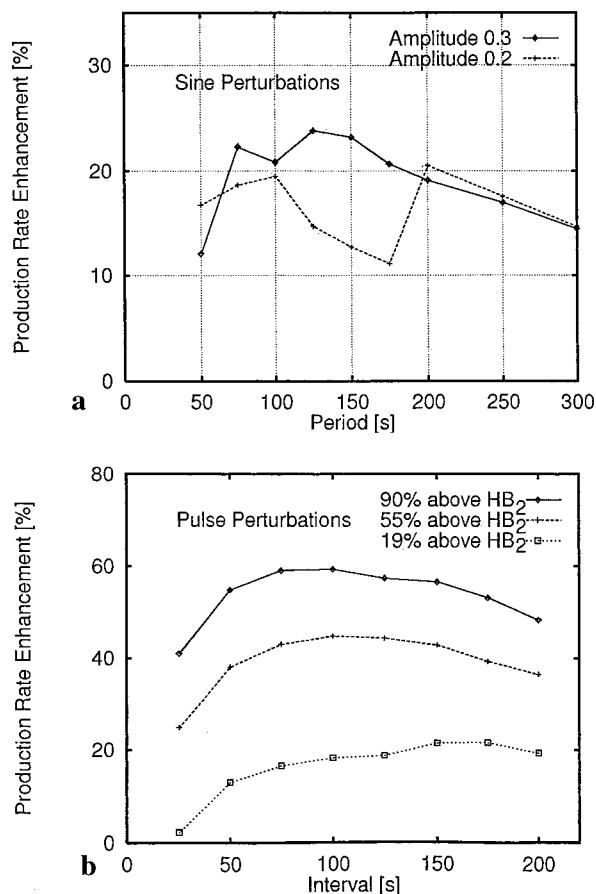


**Figure 4.** Production rate enhancement in the MB experiments (a) versus sine perturbation period at  $\alpha = 0.2$  (dotted line) and  $\alpha = 0.3$  (solid line) at  $k_f^0 = 0.0040 \text{ s}^{-1}$  and (b) versus interval time using rectangular pulse perturbations at  $k_f$  values located 19%, 55%, and 90% above  $\text{HB}_2$  on the  $\text{SS}_2$  branch at an optimal pulse length of 10 s. During each short pulse the minimum  $k_f$  value is 80% below  $\text{HB}_2$ , i.e., near zero flow rate.

production rate. In this particular case the minimal flow rate (80% below  $\text{HB}_2$ ) is smaller than in the sinusoidal case.

If the production rate enhancements are calculated at the respective flow rates of the free running system (Figure 1b) (and not at the maximal production rate in the free running mode at  $k_f = 0.0033 \text{ s}^{-1}$ ), the experimental PR rate enhancements are even higher, namely 60%, 56%, and 66% in parts b, d, and f Figure 3, respectively.

**On- and Off-Modulation of the Flow Rate.** In further pulse experiments using rectangular pulse perturbations (Figure 4b, pulse length 10 s), the maximum  $k_f$  values were located 19%, 55%, and 90% above  $\text{HB}_2$  on the  $\text{SS}_2$  branch, whereas the minimum  $k_f$  values were chosen to be 80% below  $\text{HB}_2$  (as in Figure 3e). In this series the minimal flow rate is near zero, which means it is practically switched off. This pulsed mode is another example of bang-bang control. Here, the highest average production rate enhancements measured were 22%, 45%, and 60% over the *maximum* production rate in the free running reaction, respectively, or 36%, 66%, and 101% over the PR at the *average* flow rates of the free running reaction, respectively. An example of a pulse pattern is shown in Figure 3e, where  $k_{f \text{ min}}$  is close to zero. Note that the average flow rate is similar to the experiment in Figure 3a whose pulse length is larger and PR enhancement is calculated to be smaller. The results show that  $\text{PR}_{\text{av}}$  increases with increasing  $k_f$  values above  $\text{HB}_2$  and that the maximum of the PR enhancement is shifted toward shorter pulse lengths intervals (Figure 4b), i.e., toward higher pulse frequencies. The results of pulse experiments with optimized pulse lengths generally show that relatively short pulse

**TABLE 1: NFT Model (Stage e)<sup>21</sup> and Rate Constants**

$\text{BrO}_3^- + \text{Br}^- + 2\text{H}^+ \rightarrow \text{HBrO}_2 + \text{HOBr}$	
$\text{HBrO}_2 + \text{Br}^- + \text{H}^+ \rightarrow 2\text{HOBr}$	
$\text{HOBr} + \text{Br}^- + \text{H}^+ \rightleftharpoons \text{Br}_2 + \text{H}_2\text{O}$	
$\text{BrO}_3^- + \text{HBrO}_2 + \text{H}^+ \rightleftharpoons 2\text{BrO}_2^* + \text{H}_2\text{O}$	
$\text{Ce}^{3+} + \text{BrO}_2^* + \text{H}^+ \rightleftharpoons \text{Ce}^{4+} + \text{HBrO}_2$	
$k_1 = 2.1 \text{ s}^{-1} \text{ M}^{-3}$	
$k_2 = 2.0 \times 10^9 \text{ s}^{-1} \text{ M}^{-2}$	
$k_3 = 8.0 \times 10^9 \text{ s}^{-1} \text{ M}^{-2}$	$k_{-3} = 1.1 \times 10^2 \text{ s}^{-1}$
$k_4 = 1.0 \times 10^4 \text{ s}^{-1} \text{ M}^{-2}$	$k_{-4} = 2.0 \times 10^7 \text{ s}^{-1} \text{ M}^{-1}$
$k_5 = 6.5 \times 10^5 \text{ s}^{-1} \text{ M}^{-2}$	$k_{-5} = 2.4 \times 10^7 \text{ s}^{-1} \text{ M}^{-1}$

lengths produce large production rate enhancements if the pulse amplitudes are sufficiently large to obtain a 1:1 response. The highest experimentally measured production rate enhancement in this work was 101% over the production rate at the same average flow rate in the free running mode.

**Model Simulations.** We use stage e of the well-known Noyes–Field–Thompson (NFT) model<sup>20,21</sup> in computer simulations. Very good agreement is obtained with the experiments for the parameters given in Table 1. The inflow species are  $\text{H}^+$  (1.5 M),  $\text{Ce(III)}$  ( $1.5 \times 10^{-4}$  M),  $\text{Br}^-$  ( $3.0 \times 10^{-4}$  M), and  $\text{BrO}_3^-$  (0.06 M). The model calculations lead to a similar bifurcation diagram as in Figure 1a with a supercritical  $\text{HB}_1$  at  $3.542 \times 10^{-3} \text{ s}^{-1}$  and a subcritical  $\text{HB}_2$  at  $4.337 \times 10^{-3} \text{ s}^{-1}$ . In the optimally pulsed mode there is an almost linear increase of the production rate with increasing  $k_f$  (Figure 5a). When the model simulations of the sinusoidal and the optimally pulsed modes (Figure 5a) are compared at the same average flow rate, slightly larger PR enhancements (2–5%) are obtained for the optimized sinusoidal perturbations. For example, the PR enhancements above the maximal free running PR is 25% (89%) for the optimized sinusoidal perturbations and 23% (84%) for pulsed perturbations, respectively, at  $k_f^{\text{avg}} = 0.0051 \text{ s}^{-1}$  ( $k_f^{\text{avg}} = 0.00819 \text{ s}^{-1}$ ). We note that the optimized sinusoidal perturbations require very large flow rate amplitudes, which may be difficult to achieve technically.

PR comparisons were also carried out at the same flow amplitudes in the sinusoidal and pulsed operations. In all cases the pulsed mode lead to substantially higher PR enhancements than the sinusoidal flow perturbations under the conditions of identical flow rate amplitudes. The reason is that the flow rate pulses are unsymmetrical; i.e., the reaction spends more time at the higher flow rate than at lower flow rates. Thus, for this specific case, the average flow rate is effectively higher in the pulsed mode than in the sinusoidal mode leading to higher PR enhancements. Finally, in agreement with our experiments, large flow rate enhancements may be obtained by simply turning the flow rate on and off in a periodic fashion. This turn-on/off mode (bang-bang method) leads to high PR enhancements at high average flow rates (above  $0.007 \text{ s}^{-1}$  (Figure 5a) where  $k_{f \text{ min}} = 0$ ). At the highest calculated  $k_f$  value ( $=0.0087 \text{ s}^{-1}$ ), the average production rate in the pulsed mode is  $\sim 84\%$  enhanced over the maximal production rate in the free running mode (at  $k_f = 4.1 \times 10^{-3} \text{ s}^{-1}$ ). If the pulsed production rate is compared with the production rate at the same flow rate as in the free running system, the enhancement is up to  $\sim 350\%$  (factor of 4.5 at  $k_f = 8.7 \times 10^{-3} \text{ s}^{-1}$ ) of that in the unperturbed case.

It is interesting to calculate a practical quantity, namely, the profit enhancement in threshold systems (PENTS) as the difference between the profit in the pulsed mode and the maximal profit in the free running mode (at  $k_f = 4.1 \times 10^{-3} \text{ s}^{-1}$ ). In general, the profit may be defined as the difference between the (monetary) value of the obtained product and the (monetary) value of the reactants. The value of the product per unit time is equal to the mathematical product of the average production rate, the price  $p$  per mol/L of the initial reactants ( $\text{Ce(III)}$ ), and

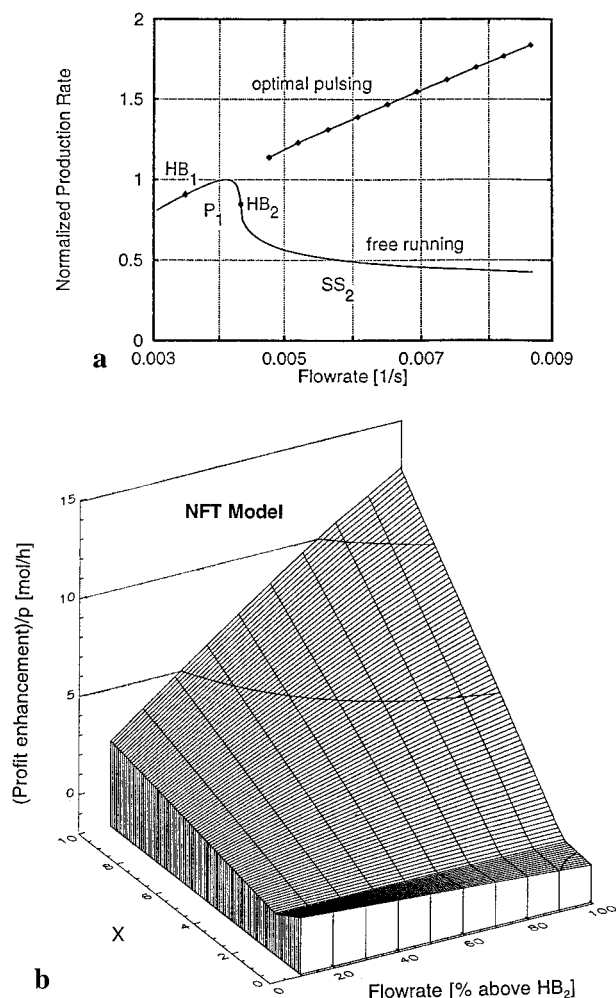


**Figure 5.** (a) NFT model production rates (normalized as in Figure 1b) versus  $k_f$  in the free running mode and in the pulsed mode (see text), where, in the pulsed mode,  $k_f$  represents the maximal flow rate. (b) Profit enhancement in threshold systems (PENTS) in the optimally pulsed mode for running the reaction in various foci located between 10% and 100% (rising lines) above HB<sub>2</sub> at increasing values of  $X$ ; optimal production rates of (a) have been used to calculate eq 3 for the NFT model. For a reactor volume of 1000 L and 1 h of running time the profit enhancement over the profit in the free running system at  $k_f = 4.1 \times 10^{-3} \text{ s}^{-1}$  has been calculated for values of  $X$  and various distances (in %) from HB<sub>2</sub>. For low values of  $X$  ( $X \sim 1.5$ ), the (low) profit enhancement is practically independent of the distance from HB<sub>2</sub>. For high values of  $X$ , it is most profitable to run the reaction at large distances from HB<sub>2</sub> (at high values of the average  $k_f$ ). For example, for  $X = 10$  and 100% (10%) above HB<sub>2</sub>, the profit enhancement is 12.5 $p$  mol/h (2.5 $p$  mol/h). Thus the higher the cost ratio  $X$ , the more PENTS. (An inspection of sales catalogs shows that the prices of Ce(III) and Ce(IV) are about equal, which indicates that Ce(IV) is produced commercially by processes other than by the present MB reaction, of course.)

the price ratio ( $X$ ) of the basic prices of [product]/[reactant]. Miscellaneous expenditures for electricity, reactor material, etc. may be included in  $X$ . The cost per unit time of the initial reactants is  $[\text{CeIII}_0]pk_f^{\text{av}}$ , where  $k_f^{\text{av}}$  is the average  $k_f$ . Thus the profit per unit time is the difference between the two terms:

$$\text{profit/time} = p/(X(\text{PR}_{\text{av}}) - [\text{CeIII}_0]k_f^{\text{av}}) \quad (3)$$

We have calculated eq 3 for the NFT model using the optimized average production rates in the pulsed mode as in Figure 5a. The quantitative results show (Figure 5b) that PENTS is optimal if the reaction is carried out at high flow rates and high price ratios  $X$  in the pulsed mode as expected.

In the present MB reaction the flow rate was chosen as a bifurcation parameter for practical reasons although other

variables may do as well. The usefulness of the production rate enhancement in large scale chemical reactions remains to be shown for industrial syntheses. To our knowledge the phenomenon of the production rate enhancement in threshold systems has not received attention so far in homogeneous chemical reactions in the liquid phase.

## Conclusions

The production rate in a reactor is maximal in the free running mode at the reaction threshold (subcritical Hopf bifurcation) in the MB reaction in which the reaction yield of Ce(IV) increases with decreasing flow rate. The production rate is dramatically enhanced for optimized short pulses of the flow rate. Sinusoidal perturbations produce slightly larger enhancements if they are compared at the same average flow rate with the pulsed perturbations. However, the sinusoidal perturbations require large flow rate amplitudes, which may be difficult to achieve technically. If the comparison is made at the same amplitudes, the pulsed mode produces larger PR enhancements than the sinusoidal operation. In the pulsed mode an optimal production rate enhancement over the free running mode has been achieved by operating at very high flow rates and simply turning the feed-pump periodically on and off, which may be easily realized in any technical applications. Calculations of the NFT model are in agreement with the experiments. The calculations show high profit enhancements in the pulsed mode at high price ratios. Production rate enhancement is not restricted to oscillatory reactions; a nonoscillatory bistability will do as well although with smaller PR enhancements.<sup>23</sup>

**Acknowledgment.** We thank Prof. M. Marek for valuable discussions and the Deutsche Forschungsgemeinschaft for financial support.

## References and Notes

- (1) Douglas, J. M.; Rippen, D. W. T. *Chem. Eng. Sci.* **1966**, *21*, 305.
- (2) Bailey, J. E. *Automatica* **1972**, *8*, 451.
- (3) Bailey, J. E. *Chem. Eng. Commun.* **1974**, *1*, 111.
- (4) For a review, see: Bailey, J. E. In *Chemical Reactor Theory A Review*; Amundson, N. R., Lapidus, L., Eds.; Prentice-Hall Inc.: Englewood Cliffs, NJ, 1977; p 758.
- (5) Rehmus, P.; Ross, J. In *Oscillations and Traveling Waves in Chemical Systems*; Field, R. J., Burger, M., Eds.; John Wiley and Sons, Inc.: New York, 1985.
- (6) Lazar, J. G.; Ross, J. *Science* **1990**, *247*, 189.
- (7) Samples, M. S.; Hung, Y. F.; Ross, J. *J. Phys. Chem.* **1992**, *96*, 7338.
- (8) Bar-Eli, K. *J. Phys. Chem.* **1985**, *89*, 2852.
- (9) Marek, M.; Schreiber, I. *Chaotic Behavior of Deterministic Dissipative Systems*; Cambridge University Press: Cambridge, 1991.
- (10) Dolnik, M.; Finkeova, J.; Schreiber, I.; Marek, M. *J. Phys. Chem.* **1989**, *93*, 2764.
- (11) Finkeova, J.; Dolnik, M.; Hrudka, B.; Marek, M. *J. Phys. Chem.* **1990**, *94*, 4110.
- (12) Förster, A.; Hauck, T.; Schneider, F. W. *J. Phys. Chem.* **1994**, *98*, 184.
- (13) Hohmann, W.; Müller J.; Schneider, F. W. *J. Chem. Soc., Faraday Trans.* **1996**, *92*, 2873.
- (14) Tyson, J. J. *J. Chem. Phys.* **1977**, *66*, 905.
- (15) For a review, see: Meron E. *Phys. Rep.* **1992**, *218*, 1.
- (16) Guderian, A.; Dechert, G.; Zeyer, K. P. W.; Schneider, F. W. *J. Phys. Chem.* **1996**, *100*, 4437.
- (17) Förster, A.; Merget, M.; Schneider, F. W. *J. Phys. Chem.* **1996**, *100*, 4442.
- (18) Hohmann, W.; Müller J.; Schneider, F. W. *J. Phys. Chem.* **1996**, *100*, 5388.
- (19) Geiseler, W.; Bar-Eli, K. *J. Phys. Chem.* **1981**, *85*, 908.
- (20) Noyes, R. M.; Field, R. J.; Thompson, R. C. *J. Am. Chem. Soc.* **1971**, *93*, 7315.
- (21) Bar-Eli, K. *J. Phys. Chem.* **1985**, *89*, 2855.
- (22) Ramirez, W. F., *Process Control and Identification*; Academic Press: New York, 1994; Chapter 8.
- (23) Schinor N.; Hohmann, W.; Kraus, M.; Schneider, F. W. To be submitted.